Growing Multihydroxyl Hyperbranched Polymers on the Surfaces of Carbon Nanotubes by in Situ Ring-Opening Polymerization

Youyong Xu,[†] Chao Gao,*[,†,‡] Hao Kong,[†] Deyue Yan,[†] Yi Zheng Jin,[‡] and Paul C. P. Watts[‡]

College of Chemistry and Chemical Engineering, Shanghai Jiao Tong University, 800 Dongchuan Road, Shanghai 200240, P. R. China, and Department of Chemistry, School of Life Sciences, University of Sussex, Brighton BN1 9QJ, UK

Received July 25, 2004; Revised Manuscript Received September 20, 2004

ABSTRACT: An in situ ring-opening polymerization strategy was employed to grow multihydroxyl dendritic macromolecules on the convex surfaces of multiwalled carbon nanotubes (MWNTs), affording novel one-dimensional (1D) molecular nanocomposites. The crude MWNTs were oxidized using 60% HNO_3 and then reacted with thionyl chloride, resulting in MWNTs functionalized with chlorocarbonyl groups (MWNT-COCl). MWNT-COCl, when reacted with an excess of glycol, produced hydroxy-functionalized MWNT supported initiators (MWNT-OH). Using the MWNT-OH as the growth supporter and $BF_3{\cdot}Et_2O$ as catalyst, multihydroxy hyperbranched polyethers—treelike macromolecules—were covalently grafted on the sidewalls and ends of MWNTs via in situ ring-opening polymerization of 3-ethyl-3-(hydroxymethyl)-oxetane (EHOX). TGA measurements showed that the weight ratio of the as-grown hyperbranched polymers on the MWNT surfaces lay in the 20−87% range. The products were characterized by FTIR, NMR, DSC, TEM, and SEM. TEM indicates that the MWNTs are enveloped evenly by the hyperbranched molecules for samples with greater polymer coatings. The as-prepared nanocomposites exhibit relatively good dispersibility in polar solvents such as methanol, ethanol, DMF, and DMSO. Because of the fact that the hyperbranched macromolecules on the MWNTs contain numerous functional hydroxy groups on their periphery, the functionalized MWNTs can be further functionalized with the merits and advantages associated with dendritic polymers, which would result in a series of fascinating novel nanomaterials and nanodevices.

Introduction

The discovery of carbon nanotubes (CNTs) opened a new chapter in nanoscience.[1] Research on CNTs attracts increasing interest nowadays due to their unique structures, excellent mechanical properties, and considerable potential applications.[2] In practice, their insolubility and weak dispersibility in common solvents and matrices have limited their applications, especially in the fields of composite materials and bottom-up hybrid nanomaterials or devices. Some scientists have focused attention on tube functionalization and modification in order to improve the solubility and surface functionality.[3] Functionalization also introduces the field of CNT-based nanochemistry. Much progress has been made in this area based on the fundamental work by Smalley[4] and Haddon.[5] To date, two methodologies, namely noncovalent and covalent, have been developed to functionalize CNTs with a variety of organic, inorganic, metallic, biochemical, and polymeric structures.[6] Generally, the linkage of small or large molecules to the CNTs by covalent methods is more stable and effective. With regard to the covalent methods, carboxylic acid groups formed at the ends, and defect sites of CNTs, are commonly used for the precursor functionalization in the formation of amine, ester, and organometallic structures.[5,7] Direct reaction of the CNT sidewalls with chemicals, for example, surface fluorination of CNTs with elemental fluorine, and direct addition of nitrenes, carbenes, and radicals to the π-systems of CNTs are other useful methods for covalent attachment.[8]

Among the various covalent CNT functionalizations, binding polymers to the CNTs is a very attractive area because the individual properties of the two materials can be combined to give one hybrid material. This can be fulfilled by "graft to" and "graft from" approaches. The former involves direct reaction of existing polymers with the carboxylic acid groups on the CNTs.[9] This approach is easy to carry out with many linear polymers having functional end groups[10] and also with low-generation dendrons with one functional group.[11] It has also been reported that using a multifunctional dendrimer, and reacting CNTs with the periphery of the dendrimer, produced star-shaped nanostructures.[12] The apparent limitation of the "graft to" approach lies in the low grafting density due to the hindrance of the pregrafted polymer chains.[13] However, on the other hand, the "graft from" approach involves in situ polymerization of monomers from the preformed initiators on the CNT surfaces, resulting in higher grafting density, and control over polymer growth with the possibility of designable structures.[14] Thus, atom transfer radical polymerization (ATRP),[9g,14,15] radical polymerization,[16] anionic polymerization,[17] and ring-opening metathesis polymerization (ROMP)[18] techniques have been adopted to covalently grow polymers on the surface of CNTs.

Until recently, most of polymers grafted to CNT surfaces have been linear. For the "graft to" polymers, many of the polymer functional groups have reacted with the carboxylic groups, which lowers the possibility of further functionalization. For the "graft-from" polymers, the monomer types used are limited to vinyl, resulting in polymer chains lacking functionality.

[†] Shanghai Jiao Tong University
[‡] University of Sussex.
* Corresponding author: e-mail chaogao@sjtu.edu.cn; Tel +86-21-54742665; Fax +86-21-54741297.

10.1021/ma0484781 CCC: $27.50
Published on Web 10/30/2004

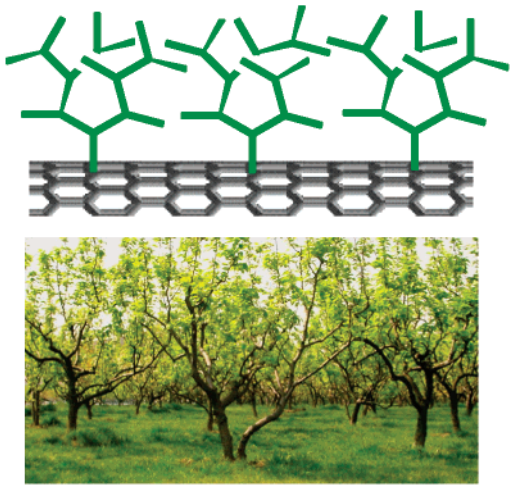

Figure 1. Graphical representation of a section of MWNT-HP nanohybrids presented in this paper (top) and a photograph of the trees grown on a hillside (bottom).

Here we report a novel "graft-from" approach based on the in situ ring-opening polymerization (ROP) to functionalize MWNTs with multihydroxyl hyperbranched polyethers. Hyperbranched polymers are globular, highly branched macromolecules with three-dimensional dendritic architecture.[19] Because of their low melting viscosity, high solubility, and abundance of functional groups, hyperbranched polymers have potential applications in wide range of fields from drug delivery to material coatings.[20] Hyperbranched polymers are also utilized to modify general surfaces such as Si/SiO_2 and colloidal gold, affording molecular tree-coated surfaces or hybrid nanoparticles.[21] It is expected that the growth of hyperbranched macromolecules on CNT surfaces not only provides a new route to highly functionalized CNTs but also retains the functionality of the end groups, which is crucial for increasing the functional complexity of the CNTs. Figure 1 shows a graphical representation of the hyperbranched macromolecules bonded-CNT hybrids. For intuitive and intelligible purposes, a photograph of the trees grown on a hillside is also shown in Figure 1.

Experimental Section

Materials. MWNTs were purchased from the Tsinghua-Nafine Nano-Powder Commercialization Engineering Centre. 3-Ethyl-3-(hydroxymethyl)oxetane (EHOX) (Aldrich, 97%) was vacuum-distilled and stored in the presence of 4 Å molecular sieves before use. Thionyl chloride ($SOCl_2$) and boron trifluoride etherate ($BF_3{\cdot}OEt_2$) were purchased from Acros and used as received. Dichloromethane (CH_2Cl_2) was boiled under reflux with CaH_2 for 24 h and distilled before use. Ethylene glycol ($HOCH_2CH_2OH$) was obtained from the Shanghai Reagents Co., previously distilled and stored in the presence of 4 Å molecular sieves in order to eliminate traces of water. Tetrahydrofuran (THF), methanol (MeOH), potassium hydroxide (KOH), and nitric acid (HNO_3) were purchased from the Shanghai Reagents Co. and used as received.

Instruments and Measurements. Fourier transform infrared (FTIR) spectra were recorded using a PE Paragon 1000 spectrometer (KBr disk). Nuclear magnetic resonance (^1H NMR and ^{13}C NMR) measurements were conducted using a Varian Mercury Plus 400 MHz spectrometer with DMSO-d_6 as the solvent. Ultraviolet−visible (UV−vis) spectra were measured using a PE Lambda 20 spectrophotometer. Molecular weight measurements were carried out in a PE series 200 gel permeation chromatograph (GPC) with polystyrene (PS) as the standard, using LiBr/DMF (0.01 mol/L) as the eluent at a flow rate of 1 mL/min. Thermal gravimetric analyses (TGA) were carried out using a PE TGA-7 instrument with a heating rate of 20 °C/min in a nitrogen flow (20 mL/min). The PE Pyres-1 model of differential scanning calorimetry (DSC) was used to measure the glass transition temperature (T_g) of the samples under nitrogen at a heating rate of 20 °C/min from −20 to 200 °C. Scanning electron microscopy (SEM) images were obtained from a LEO 1550VP microscope, and the samples were sputter-coated with a layer of homogeneous gold to facilitate charge dissipation during imaging. Transmission electron microscopy (TEM) was conducted using a JEOL JEL2010 electron microscope at 200 kV. The samples for TEM were prepared by placing one drop of sample, previously ultrasonically dispersed in acetone, on copper grids coated with lacy carbon. Atomic force microscopy (AFM) was measured by Digital Instrument Nanoscape III a SPM, operating at the tapping mode. The samples were prepared by placing a drop of dispersed functionalized MWNT in methanol on the mica surface.

Preparation of MWNT-COOH from MWNT.[14] Crude MWNTs (1.0453 g) were added to aqueous HNO_3 (10.0 mL, 60%). The mixture was placed in an ultrasonic bath (40 kHz) for 30 min and then stirred for 24 h while being boiled under reflux. The mixture was then vacuum-filtered through a 0.22 μm Millipore polycarbonate membrane and subsequently washed with distilled water until the pH of the filtrate was ca. 7. The filtered solid was dried under vacuum for 12 h at 60 °C, yielding MWNT-COOH (0.6104 g).

Generation of MWNT-COCl from MWNT-COOH. MWNT-COOH (0.6104 g) was suspended in $SOCl_2$ (20 mL) and stirred for 24 h at 65 °C. The solution was filtered, washed with anhydrous THF, and dried under vacuum at room temperature for 2 h, generating MWNT-COCl (0.5384 g).

Synthesis of MWNT-OH Initiators from MWNT-COCl. MWNT-COCl (0.5016 g) was mixed with ethylene glycol (20.0 mL) and stirred for 48 h at 120 °C. The resulting solid was separated by vacuum-filtration using 0.22 μm Millipore polycarbonate membrane filter and subsequently washed with anhydrous THF. After repeated washing and filtration, the resulting solid was dried overnight in a vacuum, generating MWNT-OH (0.4342 g).

Growth of Hyperbranched Polymers Initiated by MWNT-OH. As-prepared MWNT-OH initiator (0.1 g) was carefully dried in a 150 mL three-necked round-bottom flask in a vacuum at 80 °C. Then the flask, equipped with dropping funnel and argon inlet and outlet, was degassed by three freeze−pump−thaw cycles. CH_2Cl_2 (50 mL) and $BF_3{\cdot}OEt_2$ (1 mL) were added to the flask by syringe. The solution was placed in an ultrasonic bath (40 kHz) for 10 min, after which it was cooled to −10 °C in an ice/NaCl bath. 3-Ethyl-3-(hydroxymethyl)oxetane (EHOX, 5 mL) was added dropwise to the solution, and the mixture was stirred for 24 h. Methanol was then added in order to quench the reaction. The mixture was subsequently filtered and washed three times with methanol. To ensure that no ungrafted polymer or free reagents were present in the product, the filtered solid was redispersed in methanol, filtered, and washed three times with methanol. The product was dried overnight to give the hyperbranched polymer-grafted MWNTs (MWNT-HP6 in Table 1, 0.4 g).

Cleavage of Hyperbranched Polymers from the Functionalized MWNTs. MWNT-HP6 (0.2 g), THF (40 mL), and KOH (5 g) were placed in a round-bottom flask. The mixture was stirred and boiled under reflux at 70 °C for 72 h. The product was filtered, and the resulting filtrate was condensed and precipitated in H_2O. This was filtered and dried in vacuo, generating the cleaved hyperbranched polyether (0.12 g).

Comparative Experiments and Preparation of Mix-1 and Mix-2. Two comparative samples were obtained. The first was the mixture of MWNTs and hyperbranched polyethers with a number-average molecular weight (M_n) of 6500 and a polydispersity index (PDI) of 1.56. MWNTs (0.1 g) were added to a solution of hyperbranched polyether (0.1 g) in MeOH (10 mL), and the mixture was stirred for 24 h at room temperature. MeOH was subsequently removed by evaporation, and

Table 1. Reaction Conditions and Some Results

sample	R_{feed} (mL/g)[a]	polymer (wt %)[b]	thi (nm)[c]	$M_{n,cleaved}$[d]	$PDI_{cleaved}$	$M_{n,free}$[e]	PDI_{free}
MWNT-HP1	5:1	20.7					
MWNT-HP2	10:1	26.3					
MWNT-HP3	20:1	35.6	3.6				
MWNT-HP4	30:1	71.6	8.5	5200	1.45	3000	1.52
MWNT-HP5	40:1	74.4	9.2	5800	1.44	3200	1.55
MWNT-HP6	50:1	87.6	12.5	7500	1.41	3500	1.60

[a] The feed ratio of monomer (EHOX) (mL) and MWNT-OH (g). [b] The polymer content calculated from TGA weight loss between 250 and 450 °C. [c] The average thickness of the grafted polymer shell measured by HRTEM. [d] Number-average molecular weight of the cleaved polymers made by hydrolysis of MWNT-HP. [e] Number-average molecular weight of the free polymers collected in the polymerization system.

Scheme 1

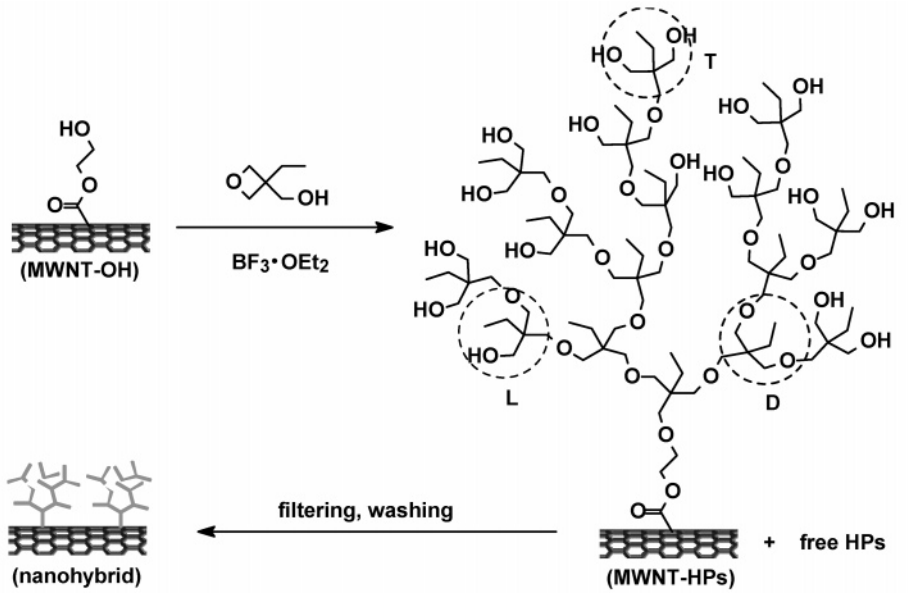

the residue was dried in vacuo, yielding the sample Mix-1. The second sample was prepared as follows: MWNT-OH (0.1 g) was added to a solution of hyperbranched polyether (0.4 g) in MeOH (12 mL), and the mixture was stirred for 24 h at room temperature. It was then filtered and washed with MeOH. After redispersing, filtering, washing, and drying, the sample Mix-2 was collected.

Results and Discussion

Preparation and Characterization of Hyperbranched Polymer-Grafted MWNTs. Scheme 1 illustrates the synthetic process for the MWNT-hyperbranched polyether (MWNT-HP) nanohybrids. The hyperbranched molecular trees were grown from the MWNT surfaces via in situ cationic ring-opening polymerization[22] of EHOX in the presence of BF_3•OEt_2. Experiments with different monomer/MWNT-OH feed ratios (R_{feed}) were conducted in order to grow hyperbranched trees of different sizes and hence various thickness on the tubes. On the other hand, the monomer, EHOX, possesses an active hydroxyl group, which can be self-initiated to form free hyperbranched polyethers (HPs) if catalyzed by BF_3•OEt_2.[22f,g] Therefore, MWNT-HPs and free HPs can exist in the same reaction system. The adsorbed HPs can be completely removed from the resulting MWNT-HP samples by successive filtering and washing. The comparative experiment showed that the possible amount of adsorbed HPs was negligible in the Mix-2 sample.

The grafted polymer content of the MWNT-HP can be calculated from TGA by the weight loss between 250 and 450 °C (Figure 2). The reaction ratio and results

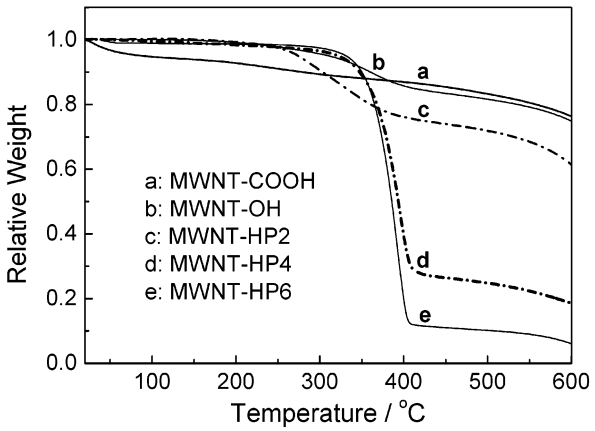

Figure 2. TGA thermograms of MWNT-COOH (a), MWNT-OH (b), MWNT-HP2 (c), MWNT-HP4 (d), and MWNT-HP6 (e).

are summarized in Table 1. For comparison, the TGA curves of MWNT-COOH and MWNT-OH are also shown in Figure 2. In the MWNT-COOH case, there was a continuous but not very obvious decrease in weight between 120 and 450 °C, which is typical for acid-functionalized MWNTs.[23] The onset of decomposition for MWNT-OH is ca. 310 °C, which is significantly higher than the boiling point of ethylene glycol. The mixed sample of crude MWNTs and ethylene glycol showed an onset temperature below 200 °C. Such a high onset temperature for MWNT-OH demonstrates that glycol is covalently linked to the MWNTs.[14]

The quantity of polymer grown on the tubes increased slightly when the R_{feed} was lower than 20/1 and in-

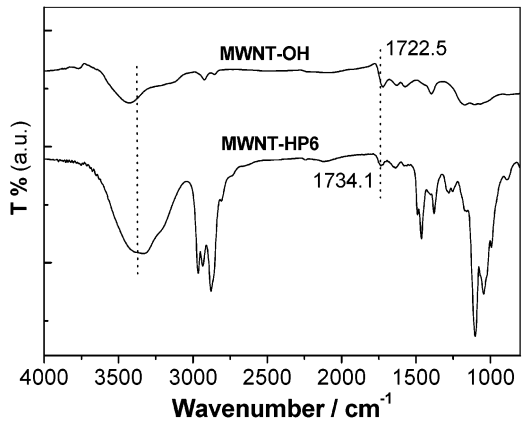

Figure 3. FTIR spectra of MWNT-OH and MWNT-HP6.

creased dramatically when the R_{feed} was in the 20/1−30/1 range. It then slightly rose again when the R_{feed} was greater than 30/1. The reason for the prominent polymer grown between 20/1 and 30/1 feed ratios is not clear to us at this stage and will be studied in the forthcoming work. The molecular weights of the grafted HPs obtained by hydrolysis of MWNT-HPs and the free HPs collected from the filtrate were also measured by GPC (Table 1). It is found that the number-average molecular weight (M_n) of the grafted HPs increased with increasing R_{feed}, while the M_n of free HPs altered little in different reactions. From the increasing tendency, we can find that the higher the feed ratio, the greater the grafted polymer amount, and the larger the molecular weight for the polymers bonded on the MWNT surfaces. In fact, this variation is similar to the synthesis of hyperbranched polymers initiated with small organic molecules. Generally, the lower the proportion of initiators, the higher the molecular weight of hyperbranched polymers.[19d,24] Thus, when the R_{feed} is lower, the relatively proportion of MWNT-supported initiators is higher, resulting in smaller molecular weight and lower grafted polymer content.

Interestingly, the M_n of the grafted HPs was higher than that of the corresponding free HPs, while the PDI is reversed, which indicates that the nanosurface-supported polymerization has lower chance of termination and cyclization than the homogeneous solution polymerization. This effect can be attributed to the fixing of one site of the grafted polymer, limiting the free movement of the molecules. On the other hand, the MWNT-OH hydroxy groups were activated by the catalyst before addition of the monomer; therefore, initial initiation would occur on the MWNTs, which may also partly contribute to the higher molecular weight for the polymers grown on the tube surfaces.

The functionalized MWNTs exhibited relatively good dispersibility/solubility in polar solvents such as methanol, ethanol, DMF, and DMSO. Dispersibility of the samples increases with the increase of the grafted polymer. UV−vis measurements showed a strong absorption for MWNT-HP6 during 200−1000 nm, which was ca. 10 times greater than that of MWNT-OH with 600 nm as the calibration point in a MeOH solution of the same sample concentration (5×10^{-5} g/mL). The higher the concentration of functionalized moieties, the stronger the absorption would be.

Figure 3 shows the FTIR spectra of MWNT-OH and MWNT-HP6. The detailed characterization of the macroinitiators (MWNT-OH), confirming covalent linkage,

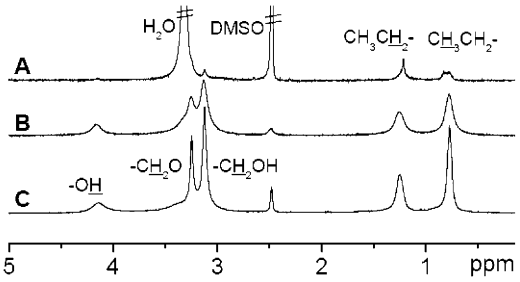

Figure 4. ^{1}H NMR spectra (DMSO-d_6) of MWNT-HP2 (A), MWNT-HP4 (B), and MWNT-HP6 (C).

Table 2. Glass Transition Temperature of the Polymers Grafted on the MWNTs and Cleaved from MWNTs

sample	T_g (°C)	ΔT_g (°C)[a]
MWNT-HP4	48.6	4.9
cleaved MWNT-HP4	43.7	
MWNT-HP5	50.3	5.1
cleaved MWNT-HP5	45.2	
MWNT-HP6	53.5	6.7
cleaved MWNT-HP6	46.8	

[a] The difference between the T_gs of the polymers grafted on the MWNTs and cleaved from MWNTs.

has been described previously.[14] The carbonyl bonds (C═O) assigned to MWNT-OH and MWNT-HP6 occur at 1722.5 and 1734.1 cm^{-1}, respectively. The obvious features are the much stronger bands at 3200−3750 cm^{-1} (ν_{O-H}) and 2750−3100 cm^{-1} (ν_{C-H}) for the MWNT-HP6, which corroborates with the structure of the grafted polymer on MWNTs. Other MWNT-HP samples showed similar characteristic bands.

The structure of the MWNT-HPs was further analyzed by NMR spectroscopy. Figure 4 shows the ^{1}H NMR spectra. For the samples with a lower quantity of grafted polymer (e.g., MWNT-HP2) the polymer unit signals were very weak because of its relatively low solubility. The H_2O peak covers the peak assigned to the $-CH_2O-$ structure. The signals became stronger for the samples with higher grafted polymer (e.g., MWNT-HP4 and MWNT-HP6). The hydrogen peaks of the grafted polymer units (e.g., CH_3-, $-CH_2-$, $-CH_2OH$, $-CH_2O-$, and $OH-$) are clearly observed in the corresponding ^{1}H NMR spectrum. ^{13}C NMR spectra of polymers cleaved from MWNT-HPs were also used to characterize the structure of the grafted polymers and will be discussed in the following section.

Chain Flexibility of the Grafted Hyperbranched Macromolecules. The linear polymer chains generally become more rigid after linking on the surface of MWNTs, as confirmed by the increase in glass transition temperature (T_g).[15a,23a] This gives rise to questions regarding the hyperbranched polymers. Therefore, DSC measurements on the MWNT-HP samples and the degrafted HPs were conducted. The corresponding T_gs are listed in Table 2. The T_g of HPs linked to the MWNTs is ca. 5−7 °C higher than that of cleaved HPs, which indicates that the covalent linkage of hyperbranched polymer to the surface has influenced the chains' flexibility, but not as significantly as some linear polymers have.[23a] Linear polystyrenes linked to MWNT surfaces show a 10−20 °C higher T_g than the cleaved polymer.[23a] In the HP case, only one point is fixed to the MWNT surface, so there are effectively tens of free terminal units with little to no entanglement existing among the macromolecules. Thus, the effect of chain flexibility is not prominent. However, for the linear

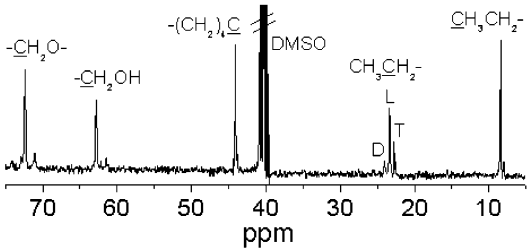

Figure 5. Quantitative ^{13}C NMR spectrum (DMSO-d_6) of the hyperbranched polyethers cleaved from MWNT-HP6.

Table 3. Degree of Branching of the Cleaved Hyperbranched Polymers from the Surface of MWNTs (DB_{tree}) and Degree of Branching of the Free Hyperbranched Polymers in the Solution (DB_{free})

		^{13}C NMR relative intensity, %				
R_{feed}	HPs[a]	T	L	D	DB_{tree}	DB_{free}
30:1	1_{NT}	15.32	75.15	9.63	0.25	
	1_{free}	24.62	65.25	10.12		0.35
40:1	2_{NT}	18.92	69.88	11.20	0.30	
	2_{free}	25.94	66.09	7.97		0.34
50:1	3_{NT}	25.95	57.98	16.07	0.42	
	3_{free}	30.81	56.68	12.51		0.43

[a] The footnotes of "NT" and "free" designate the hyperbranched polymers (HPs) cleaved from MWNTs and free HPs in the solution, respectively.

polymers, there are only two terminal units, one of which is fixed. Therefore, for high-density grafted MWNTs, high molar mass polymer chains will entangle easily, so the effect on flexibility will always be stronger.

Topology of the Grown Hyperbranched Molecular Trees. The topology of hyperbranched polymers is mainly dependent on the following criteria: degree of branching (DB), molecular weight (MW), and unit density (or the distance between two neighboring dendritic units).[20a−c] For a specific hyperbranched macromolecule with known MW, the DB is the most important parameter in characterizing its topological structure.[24] A hyperbranched polymer generally contains dendritic units (D), linear units (L), terminal units (T), and one initial unit (I) (see Scheme 1). In the experimental, the DB can be calculated using Fréchet's equation:[25]

$$DB = (D + T)/(D + T + L) \quad (1)$$

In the case of the hyperbranched molecular trees grown on the MWNT surfaces, the DB was obtained from quantitative (inverse-gated) ^{13}C NMR spectra.[22f] Figure 5 shows the quantitative ^{13}C NMR spectrum of the cleaved HPs from MWNT-HP6. The carbon signals of CH_3CH_2-, $C(CH_2)_4-$, $-CH_2OH$, and $-CH_2OCH_2-$ appeared at $\delta = 8.4$, 44, 62.9, and 72.3 ppm, respectively. Three adjacent peaks are found at 22.6, 23.3, and 23.9 ppm, which are assigned to the CH_3CH_2- carbon signals corresponding to the terminal, linear, and dendritic units, respectively. From the relative integration value of the three peaks, the DB is easily calculated using eq 1.[26] For comparison, the DBs of the cleaved and free HPs were measured and are summarized in Table 3. It is apparent that the DB increases with increasing MW for cleaved and free HPs, which accords with the theoretical prediction.[24b,27] Interestingly, the DB of the cleaved HPs (DB_{tree}) is lower than that of the free HPs (DB_{free}) although the cleaved HPs have a larger M_n, and the smaller the molecular weight, the higher the disparity ($\Delta DB = DB_{free} - DB_{tree}$). This may be attributed to steric hindrance of the grafted molecules; the smaller the molecular weight, the stronger the hindrance effect because of the limited space. For the MWNT-HP6 sample, the DB of the grafted trees is 0.42.[26] This value is almost equal to the DB of free HPs, which approaches the maximum (<0.45, typical 0.43−0.44) that this particular hyperbranched polyether can achieve in our experiments. Therefore, molecular trees with a high DB can be grown on MWNT surfaces via the in situ ring-opening polymerization.

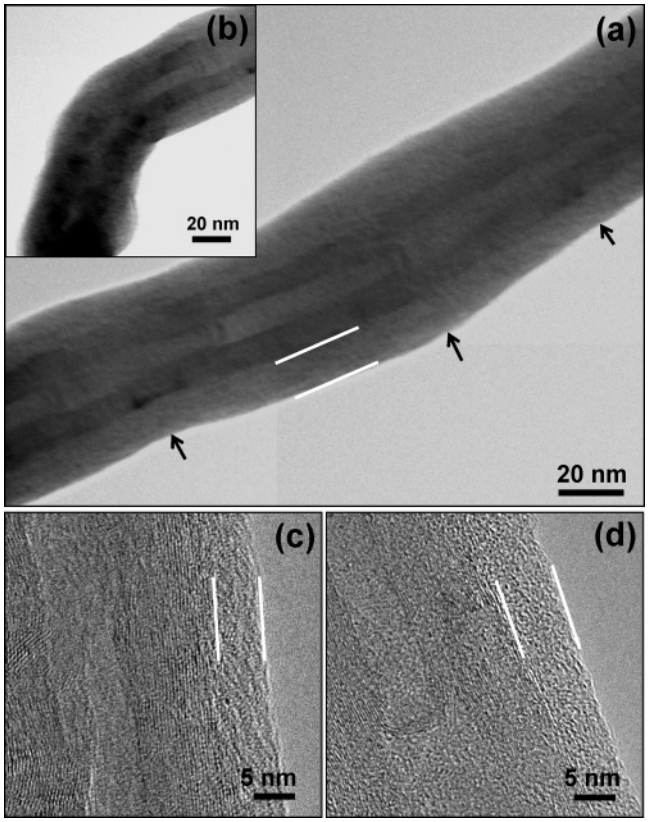

Figure 6. TEM images of MWNT-HP6.

Structure of the Molecular Nanohybrids. TEM, especially high-resolution TEM (HRTEM), is a powerful tool for characterizing nanomaterials such as CNTs and polymer-functionalized CNTs.[13,14] Using HRTEM, core−shell structures of polymer-grafted MWNTs are easily observed, and the thickness of the polymer shell can be measured according to our previous work.[14,28] TEM and HRTEM were also used to view the molecular structure of the MWNT-HP nanohybrids. Figure 6 shows the typical HRTEM images of MWNT-HP6. The core−shell structure of the 1D nanohybrids is clearly observed. At the MWNTs' surface, the hyperbranched molecular trees were grown with high density. For some nanotubes reported previously,[29] the ends and bends exhibited more defects mainly because of the existence of more pentagons and heptagons. They then showed more reactivity. Therefore, these tubes can be locally functionalized. By contrast, where the bends or ends of our MWNTs (one tube bend is shown in Figure 6, image b), the polymer layer has almost the same thickness as the rest of the tube, which indicates that the initiation sites or the defect density at the surface is even. Otherwise, the polymer layer at the bends and ends should be thicker than the straight section of the tube. On the other hand, the diameter of the same functionalized MWNT is not constant but instead varies according to

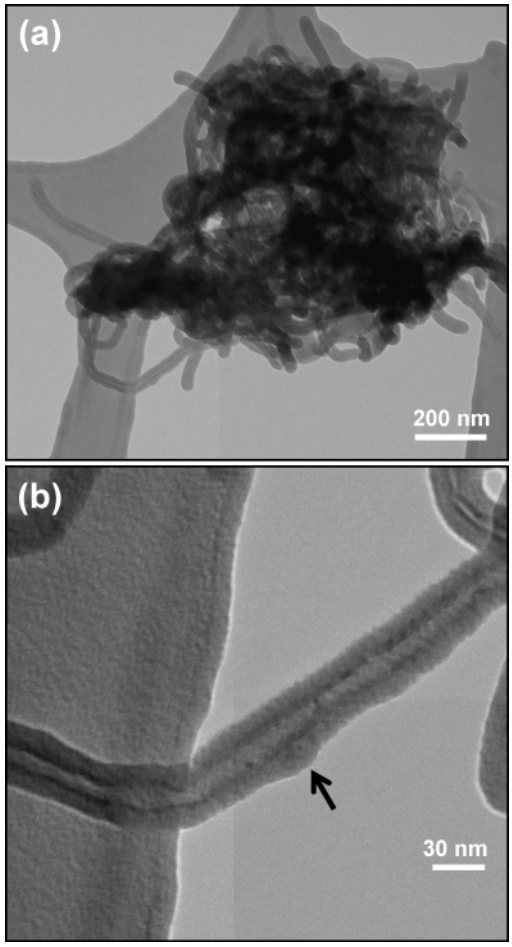

Figure 7. TEM images of MWNT-HP5 at low magnification (a) and high magnification (b).

the diameter of the MWNT and the thickness of the local polymer shell (different diameter points are marked by the arrows in Figure 6a). The thickness of the HP shell shown in Figure 6a is ca. 12−18 nm. For the tubes grafted with a thinner polymer layer, the sheet structure of graphite is detected at a higher magnification (see Figure 6, images c and d). The thickness of the HP shell shown in parts c and d of Figure 6 is ca. 6−8 and ca. 7−10 nm, respectively. It is found that the higher the grafted polymer quantity, the thicker the polymer shell. The average thickness of the grafted polymer layer for some samples, measured by HRTEM (8−12 tubes), is listed in Table 1.

Figure 7 shows TEM images of the MWNT-HP5 sample. Estimating from the low magnification image (Figure 7a), the molecular trees were also planted, or grafted, evenly to the tube surfaces. At a high magnification, the molecular trees grown on the tube surfaces are clearly observed. Again, the diameter of the nanoforests varies with the diameter of the MWNT and the grafted HPs. As marked by the arrow (Figure 7b), some tubers were observed on the surface of the MWNTs.

For comparison, the hyperbranched polyether was blended with MWNTs (sample Mix-1). Two individual phases were identified: the polymer, marked by white arrows, and MWNTs, marked by a black arrow (Figure 8a). In the HRTEM image (Figure 8b), the adsorbed polymer layer on the MWNT is difficult to detect. The MWNT surface in sample Mix-1 is the same as that of crude MWNTs.

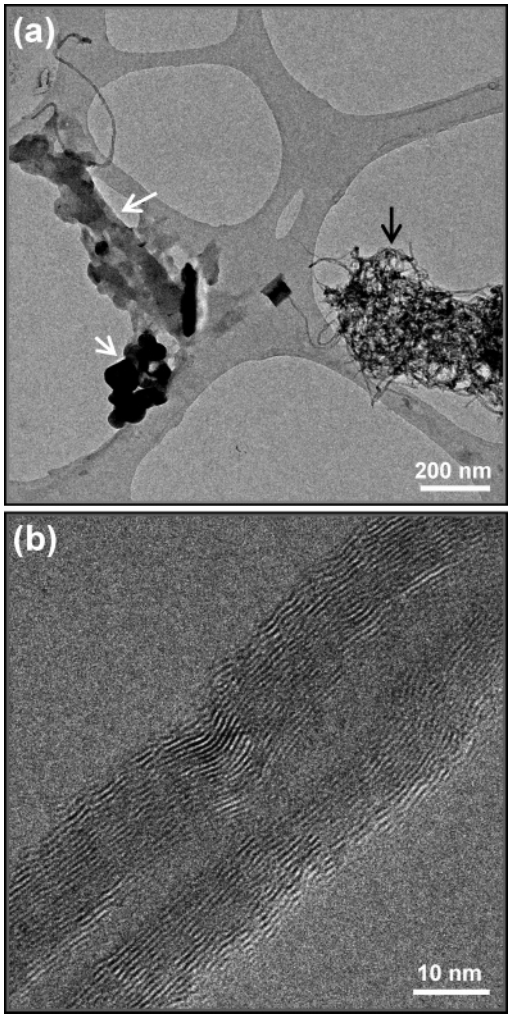

Figure 8. TEM images of sample Mix-1 (mixture of hyperbranched polyether and crude MWNTs) at low magnification (a) and high magnification (b).

Morphology of the MWNT-HP Molecular Nanohybrids. The morphologies of the molecular nanohybrids were characterized using SEM and AFM. Figure 9 shows the representative SEM images of MWNT-HP6 (a), MWNT-HP5 (b), MWNT-HP4 (c), and crude MWNTs (d). When the grafted polymer content exceeds ca. 50 wt %, the hybrid material appears to be a continuous phase (see Figure 9, images a−c). Interestingly, some protuberances were observed in the SEM image of sample MWNT-HP5 (Figure 9b), indicating a globular topology of the grafted molecular trees.

AFM measurements also demonstrated that the polymer was coated on the convex surfaces of MWNTs, and some wormlike structure and many protuberances were observed (see Figure 10). This interesting morphology was accorded with the SEM observations and in agreement with the molecular characteristics of the dendritic polymers grafted on the MWNTs.

Conclusions

Multihydroxyl hyperbranched molecular trees were successfully grown on the surface of MWNTs by in situ ring-opening polymerization of 3-ethyl-3-(hydroxymethyl)oxetane (EHOX). The hybrid material, hyperbranched macromolecules-grafted MWNTs, is described as molecular nanohybrid. The amount of polymer grafted is controllable in the range ca. 87−20 wt %. The

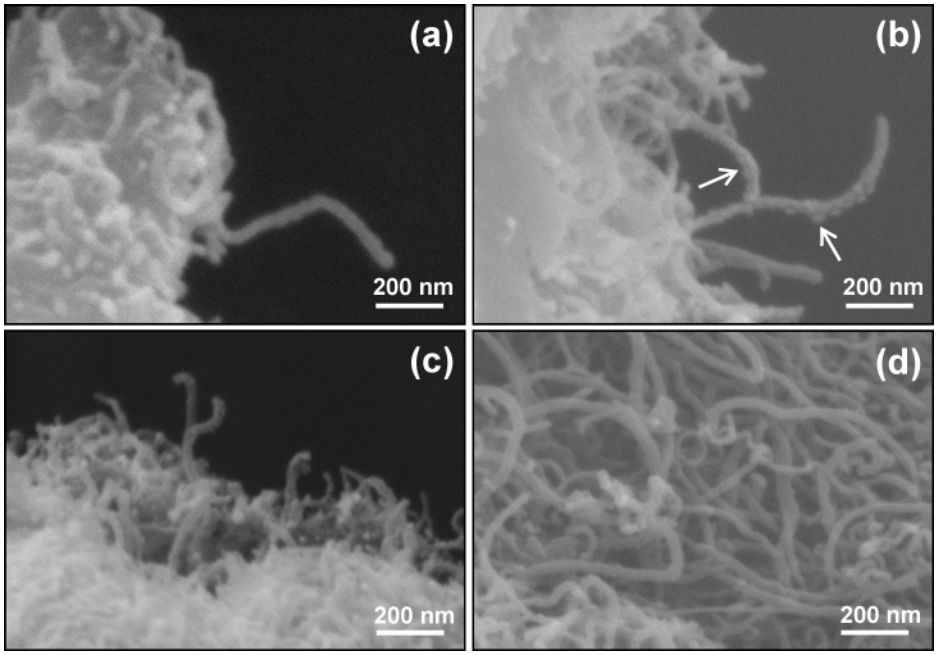

Figure 9. SEM images of MWNT-HP6 (a), MWNT-HP5 (b), MWNT-HP4 (c), and crude MWNTs (d).

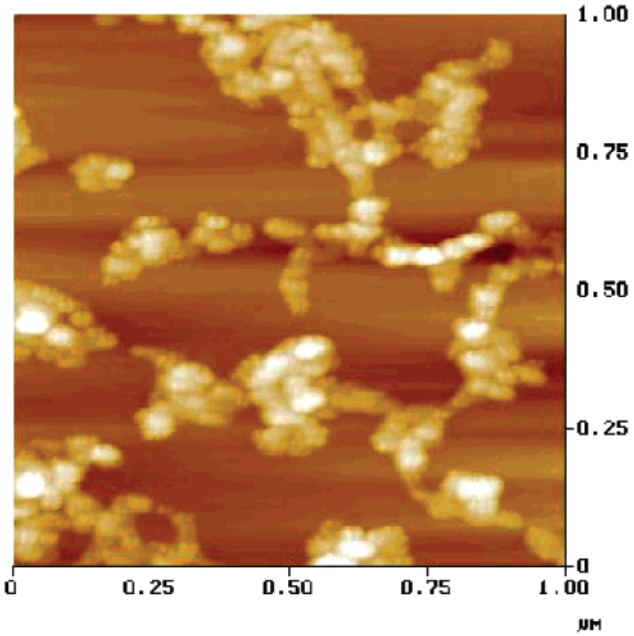

Figure 10. A representative AFM image of MWNT-HP6.

molecular weight of the grafted hyperbranched polymer increases with increasing feed ratios of the monomer (EHOX) to MWNT-supported macroinitiators (MWNT-OH). Increasing the molecular weight dramatically increases the DB of the grafted polymers, which peaked at 0.42 in our experiments. The structure and morphology of the as-prepared molecular nanohybrids were fully investigated and characterized using FTIR, NMR, TEM, SEM, and AFM, which revealed the features of covalent linkage between the hyperbranched polymers and MWNT surface. The adsorbed polymers can be easily removed by washing with solvent. If the polymer was mixed with MWNTs, the individual phases of both polymer and MWNTs are observed under TEM. No polymer layer was found on the MWNT surface at higher resolutions for the mixture.

This in situ ring-opening polymerization (ROP) approach can be easily extended to other ROP-active ring monomers and even copolymerization, grafting a series of linear and dendritic polymers onto the MWNT surfaces. Furthermore, depending on the numerous functional hydroxyl groups possessed by the molecular trees, additional functionalization, based on the molecular nanoforests, can be easily achieved. Thus, the advanced functions of dendritic polymers can be grafted to MWNTs, leading to a variety of new nanomaterials and nanodevices. Expanding work is currently in progress and will be published soon. We believe that the generality and simplicity of the synthesis strategy and the versatility and availability of the hybrid materials will further advancements in the exploration, design, fabrication, and applications of carbon nanotube-based materials.

Acknowledgment. Financial support of this work from the National Natural Science Foundation of China (Nos. 20304007 and 50473010) and Yok Ying Tung Education Foundation (No. 91013) is gratefully acknowledged. Dr. David Walton, Prof. Sir Harry Kroto, and Ms. Gill Watson are thanked for discussions on this work.

References and Notes

(1) (a) Iijima, S. *Nature (London)* **1991**, *354*, 56−58. (b) Iijima, S.; Ichihashi, T. *Nature (London)* **1993**, *363*, 603−605.

(2) For example, see: (a) Ajayan, P. M. *Chem. Rev.* **1999**, *99*, 1787−1799. (b) Dai, H. *Acc. Chem. Res.* **2002**, *35*, 1035−1044. (c) Hirsch, A. *Angew. Chem., Int. Ed.* **2002**, *41*, 1853−1859. (d) Watts, P. C. P.; Hsu, W.-K.; Barnes, A.; Chambers, B. *Adv. Mater.* **2003**, *15*, 600−603. (e) Dalton, A. B.; Collins, S.; Razal, J.; Munoz, E.; Ebron, V. H.; Kim, B. G.; Coleman, J. N.; Ferraris, J. P.; Baughman, R. H. *J. Mater. Chem.* **2004**, *14*, 1−3. (f) Popov, V. N. *Mater. Sci. Eng. R* **2004**, *43*, 61−102. (g) Thess, A.; Lee, R.; Nikolaev, P.; Dai, H.; Petit, P.; Robert, J.; Xu, C.; Lee, Y. H.; Kim, S. G.; Rinzler, A. G.; Colbert, D. T.; Scuseria, G. E.; Tomanek, D.; Fischer, J. E.; Smalley, R. E. *Science* **1996**, *273*, 483−487.

(3) For example, see: (a) Tasis, D.; Tagmatarchis, N.; Georgakilas, V.; Prato, M. *Chem.—Eur. J.* **2003**, *9*, 4000−4008. (b) Star, A.; Stoddart, J. F. *Macromolecules* **2002**, *35*, 7516−7520.

(4) Liu, J.; Rinzler, A. G.; Dai, H. J.; Hafner, J. H.; Bradley, R. K.; Boul, P. J.; Lu, A.; Iverson, T.; Shelimov, K.; Huffman, C. B.; Rodriguez-Macias, F.; Shon, Y. S.; Lee, T. R.; Colbert, D. T.; Smalley, R. E. *Science* **1998**, *280*, 1253−1256.

(5) Chen, J.; Hamon, M. A.; Hu, H.; Chen, Y.; Rao, A. M.; Eklund, P. C.; Haddon, R. C. *Science* **1998**, *282*, 95−98.
(6) For example, see: (a) Kang, Y.; Taton, T. A. *J. Am. Chem. Soc.* **2003**, *125*, 5650−5651. (b) Carrillo, A.; Swartz, J. A.; Gamba, J. M.; Kane, R. S. *Nano Lett.* **2003**, *3*, 1437−1440. (c) Besteman, K.; Lee J.-O.; Wiertz, F. G. M.; Heering, H. A.; Dekker, C. *Nano Lett.* **2003**, *3*, 727−730. (d) Rege, K.; Raravikar, N. R.; Kim, D.-Y.; Schadler, L. S.; Ajayan, P. M.; Dordick, J. S. *Nano Lett.* **2003**, *3*, 829−832. (e) Banerjee, S.; Kahn, M. G. C.; Wong, S. S. *Chem.−Eur. J.* **2003**, *9*, 1898−1908.
(7) (a) Hamon, M. A.; Chen, J.; Hu, H.; Chen, Y.; Itkis, M. E.; Rao, A. M.; Eklund, P. C.; Haddon, R. E. *Adv. Mater.* **1999**, *11*, 834−840. (b) Riggs, J. E.; Guo, Z.; Carroll, D. L.; Sun, Y.-P. *J. Am. Chem. Soc.* **2000**, *122*, 5879−5880. (c) Sano, M.; Kamino, A.; Okamura, J.; Shinkai, S. *Langmuir* **2001**, *17*, 5125−5128.
(8) (a) Mickelson, E. T.; Chiang, I. W.; Zimmerman, J. L.; Boul, P. J.; Lozano, J.; Liu, J.; Smalley, R. E.; Hauge, R. H.; Margrave, J. L. *J. Phys. Chem. B* **1999**, *103*, 4318−4322. (b) Holzinger, M.; Vostrowsky, O.; Hirsh, A.; Hennrich, F.; Kappes, M.; Weiss, R.; Jellen, F. *Angew. Chem., Int. Ed.* **2001**, *40*, 4002−4005. (c) Tagmatarchis, N.; Prato, M. *J. Mater. Chem.* **2004**, *14*, 437−439.
(9) For papers on the "grafting to" approach, for example, see: (a) Sun, Y.-P.; Fu, K.; Lin, Y.; Huang, W. *Acc. Chem. Res.* **2002**, *35*, 1096−1104. (b) Niyogi, S.; Hamon, M. A.; Hu, H.; Zhao, B.; Bhowmik, P.; Sen, R.; Itkis, M. E.; Haddon, R. C. *Acc. Chem. Res.* **2002**, *35*, 1105−1113. (c) Lin, Y.; Rao, A. M.; Sadanadan, B.; Kenik, E. A.; Sun Y.-P. *J. Phys. Chem. B* **2002**, *106*, 1294−1298. (d) Czerw, R.; Guo, Z.; Ajayan, P. M.; Sun Y.-P.; Carroll, D. L. *Nano Lett.* **2001**, *1*, 423−427. (e) Huang, W.; Taylor, S.; Fu, K.; Lin, Y.; Zhang, D.; Hanks, T. W.; Rao, A. M.; Sun, Y.-P. *Nano Lett.* **2002**, *2*, 311−314. (f) Huang, W.; Lin, Y.; Taylor, S.; Gaillard, J.; Rao, A. M.; Sun, Y.-P. *Nano Lett.* **2002**, *2*, 231−234. (g) Qin, S.; Qin, D.; Ford, W. T.; Resasco, D. E.; Herrera, J. E. *Macromolecules* **2004**, *37*, 752−757. (h) Lin, Y.; Zhou, B.; Shiral Fernando, K. A.; Liu, P.; Allard, L. F.; Sun, Y.-P. *Macromolecules* **2003**, *36*, 7199−7204. (i) Hill, D. E.; Lin, Y.; Rao, A. M.; Allard, L. F.; Sun, Y.-P. *Macromolecules* **2002**, *35*, 9466−9471.
(10) Fu, K.; Kitaygorodskiy, A.; Rao, A. M.; Sun, Y.-P. *Nano Lett.* **2002**, *2*, 1165−1168.
(11) Fu, K.; Huang, W.; Lin, Y.; Riddle, L. A.; Carroll, D. L.; Sun, Y.-P. *Nano Lett.* **2001**, *1*, 439−441.
(12) Sano, M.; Kamino, A.; Shinkai, S. *Angew. Chem., Int. Ed.* **2001**, *40*, 4661−4663.
(13) Zhao, B.; Hu, H.; Haddon, R. C. *Adv. Funct. Mater.* **2004**, *14*, 71−76.
(14) Kong, H.; Gao, C.; Yan, D. *J. Am. Chem. Soc.* **2004**, *126*, 412−413.
(15) (a) Yao, Z.; Braidy, N.; Botton, G. A.; Adronov, A. *J. Am. Chem. Soc.* **2003**, *125*, 16015−16024. (b) Qin, S.; Qin, D.; Ford, W. T.; Resasco, D. E.; Herrera, J. E. *J. Am. Chem. Soc.* **2004**, *126*, 170−176.
(16) Shaffer, M. S.; Koziol, K. *Chem. Commun.* **2002**, 2074−2075.
(17) (a) Viswanathan, G.; Chakrapani, N.; Yang, H.; Wei, B.; Chung, H.; Cho, K.; Ryu, C. Y.; Ajayan, P. M. *J. Am. Chem. Soc.* **2003**, *125*, 9258−9259. (b) Liu, I.; Huang, H.; Chang, C.; Tsai, H.; Hsu, C.; Tsiang, R. C. *Macromolecules* **2004**, *37*, 283−287. (c) Wu, W.; Zhang, S.; Li, Y.; Li, J.; Liu, L.; Qin, Y.; Guo, Z.-X.; Dai, L.; Ye, C.; Zhu, D. *Macromolecules* **2003**, *36*, 6286−6288.
(18) Liu, Y. Q.; Adronov, A. *Macromolecules* **2004**, *37*, 4755−4760.
(19) (a) Flory, P. J. *J. Am. Chem. Soc.* **1952**, *74*, 2718−2723. (b) Kim, Y. H.; Webster, O. W. *J. Am. Chem. Soc.* **1990**, *112*, 4592−4593. (c) Kim, Y. H.; Webster, O. W. *Macromolecules* **1992**, *25*, 5561−5572. (d) Kim, Y. H. *J. Polym. Sci., Part A: Polym. Chem.* **1998**, *36*, 1685−1698. (e) Xu, Y.; Gao, C.; Kong, H.; Yan, D.; Luo, P.; Li, W.; Mai, Y. *Macromolecules* **2004**, *37*, 6264−6267.
(20) For relevant reviews, for example, see: (a) Gao, C.; Yan, D. *Prog. Polym. Sci.* **2004**, *29*, 183−275. (b) Jikei, M.; Kakimoto, M. *Prog. Polym. Sci.* **2001**, *26*, 1233−1285. (c) Inoue, K. *Prog. Polym. Sci.* **2000**, *25*, 453−571. (d) Voit, B. *J. Polym. Sci., Part A: Polym. Chem.* **2000**, *38*, 2505−2525. (e) Hult, A.; Johansson, M.; Malmström, E. *Adv. Polym. Sci.* **1999**, *143*, 1−34. (f) Hawker, C. J. *Adv. Polym. Sci.* **1999**, *147*, 113−160.
(21) For example, see: (a) Mori, H.; Müller, A. H. E. *Top. Curr. Chem.* **2003**, *228*, 1−37. (b) Mori, H.; Seng, D. C.; Zhang, M. F.; Müller, A. H. E. *Langmuir* **2002**, *18*, 3682−3693. (c) Mori, H.; Boker, A.; Krausch, G.; Müller, A. H. E. *Macromolecules* **2001**, *34*, 6871−6882. (d) Khan, M.; Huck, W. T. S. *Macromolecules* **2003**, *36*, 5088−5093. (e) Tsubokawa, N.; Hayashi, S.; Nishimura, J. *Prog. Org. Coat.* **2002**, *44*, 69−74. (f) Bergbreiter, D. E.; Tao, G. L.; Franchina, J. G.; Sussman, L. *Macromolecules* **2001**, *34*, 3018−3023.
(22) For papers related to ring-opening polymerization, for example, see: (a) Magnusson, H.; Malmström, E.; Hult, A. *Macromol. Rapid Commun.* **1999**, *20*, 453−457. (b) Magnusson, H.; Malmström, E.; Hult, A. *Macromelocules* **2001**, *34*, 5786−5791. (c) Bednarek, M.; Biedron, T.; Helinski, J.; Kaluzynski, K.; Kubisa, P.; Penczek, S. *Macromol. Rapid Commun.* **1999**, *20*, 369−372. (d) Bednarek, M.; Kubisa, P.; Penczek, S. *Macromolecules* **2001**, *34*, 5112−5119. (e) Yan, D.; Hou, J.; Zhu, X.; Kosman, J. J.; Wu, H. S. *Macromol. Rapid Commun.* **2000**, *21*, 557−561. (f) Mai, Y.; Zhou, Y.; Yan, D.; Lu, H. *Macromolecules* **2003**, *69*, 9667−9669. (g) Yan, D.; Zhou, Y.; Hou, J. *Science* **2004**, *303*, 65−67.
(23) (a) Kong, H.; Gao, C.; Yan, D. *Macromolecules* **2004**, *37*, 4022−4030. (b) Kong, H.; Gao, C.; Yan, D. *J. Mater. Chem.* **2004**, *14*, 1401−1405.
(24) (a) Sunder, A.; Hanselmann, R.; Frey, H.; Mülhaupt, R. *Macromolecules* **1999**, *32*, 4240−4246. (b) Holter, D.; Burgath, A.; Frey, H. *Acta Polym.* **1997**, *48*, 30−35. (c) Holter, D.; Frey, H. *Acta Polym.* **1997**, *48*, 298−309. (d) Gao, C.; Yan, D.; Chen, W. *Macromol. Rapid Commun.* **2002**, *23*, 465−469.
(25) Hawker, C. J.; Lee, R.; Fréchet, J. M. J. *J. Am. Chem. Soc.* **1991**, *113*, 4583−4588.
(26) For instance, the relative integration values of T, L, and D units for the hyperbranched polyether cleaved from MWNT-HP6 are 0.2595, 0.5798, and 0.1607, respectively. Thus, DB = (D + T)/(D + T + L) = (0.1607 + 0.2595)/(0.1607 + 0.2595 + 0.5798) = 0.4202 ≈ 0.42.
(27) Yan, D.; Müller, A. H. E.; Matyjaszewski, K. *Macromolecules* **1997**, *30*, 7024−7033.
(28) Kong, H.; Li, W.; Gao, C.; Yan, D.; Jin, Y.; Walton, D. R. M.; Kroto, H. W. *Macromolecules* **2004**, *37*, 6683−6686.
(29) For example: (a) Chiu, P. W.; Duesberg, G. S.; Dettlaff-Weglikowska, U.; Roth, S. *Appl. Phys. Lett.* **2002**, *80*, 3811−3813. (b) Dettlaff-Weglikowska, U.; Benoit, J. M.; Chiu, P. W.; Graupner, R.; Lebedkin, S.; Roth, S. *Curr. Appl. Phys.* **2002**, *2*, 497−501. (c) Sano, M.; Kamino, A.; Okamura, J.; Shinkai, S. *Science* **2001**, *293*, 1299−1301.

MA0484781